Proceedings of the 41st Chinese Control Conference
July 25-27, 2022, Hefei, China

# Adaptive Quasi-Sliding Mode Tracking Control for Quadrotors with Input Saturation

Hujie Wei, Yan Jiang, Shixian Luo
College of Electrical Engineering, Guangxi University, Nanning 530004, P. R. China
E-mail: yanjiang986@126.com

**Abstract:** This paper focuses on the robust adaptive tracking control problem of quadrotors with input saturation. The dynamic of the quadrotors is first decoupled into position and attitude models with unknown bounded uncertainties. An adaptive quasi-sliding mode control (AQSMC) strategy is designed to perform the position and attitude tracking control, in which the adaptive laws are designed to estimate the unknown saturation errors between the original inputs and the saturated inputs. It is shown with the Lyapunov direct method that all the signals of the closed-loop system are bounded, and the tracking errors converge to zero asymptotically. The advantage of the proposed control scheme is that the AQSMC suppresses sliding mode chattering and ensures the system tracks the target stably when the input is limited. Finally, simulation results verify the effectiveness of the AQSMC algorithm.

**Key Words:** Quadrotor, Tracking Control, Sliding Mode Control, Input Saturation

## 1 Introduction

As a class of important multi-rotor saucer-shaped aircraft, quadrotors are vertical take-off and landing vehicles that can overcome their gravity by aerodynamics and fly manually or automatically, which is rifely employed in military industries and civil fields under their simple structure, flexible operation, and strong load capacity. Quadrotors can be used for rescue, reconnaissance, anti-terrorism, surveying, and mapping tasks and can replace humans in harsh environments to reduce casualties [1]. There are many challenging problems for quadrotors, such as mechanical modeling and control design. Particularly, the quadrotor is very sensitive to external disturbances and system parameters due to underactuation, strong coupling, and nonlinearity [2]. Many scholars have recently applied novel control algorithms to the quadrotor platform and achieved good results. For examples, a backstepping idea based on fuzzy neural network is employed to solve the nonlinear control problem for quadrotor systems in [3]; In [4], a self-tuning regulator acts as a quadrotor inner loop attitude adaptive tracker to better respond to parameter variations.

On the other hand, as a nonlinear dynamic control, sliding mode control forces the system to move from the current state to the set sliding mode surface until the system state reaches the origin in a finite time and stays at the origin all the time [5]. The design of sliding mode control has the advantage of insensitivity to external disturbance and parameters, and such a system also has the advantage of a fast response. Therefore, sliding mode control in aerospace and flight guidance is worth researching. For examples, nonsingular terminal sliding mode control was applied to achieve distributed formation of multi-quadrotors [6]. In [7], an anti-saturation SMC strategy was taken into account in interactive spacecraft maneuvers; the authors of [8] proposed an adaptive fuzzy terminal SMC strategy for tracking control of quadrotors. Besides, an adaptive fuzzy SMC method was adopted for the servo system [9, 10]. An adaptive integral SMC using a fully connected recurrent neural network was proposed in [11]. However, due to the discontinuity of control, sliding mode control produces chattering. Chattering can destroy the dynamic quality of SMC, and eliminating chattering is a serious challenge [12].

The main contributions of this paper are twofold: 1) an adaptive quasi-sliding mode controller is designed for quadrotors with input saturation, which reduces the chattering of conventional sliding mode control (CSMC) and ensures the control precision and speed; 2) the stability and the tracking performance of the closed-loop system are analyzed. Furthermore, the proposed method solves the problem that the quadrotor can not generate high gain control input in reality.

The rest of this paper is made up as follows: Section 2 gives the derivation and simplification of the quadrotor 6-DOF model. The design of AQSMC for the position and attitude models is presented in section 3. Section 4 demonstrates the results by simulation. Finally, the conclusions are discussed in section 5.

## 2 Quadrotor 6-DOF Model

### 2.1 Normal definitions and assumptions

In this paper, we use a cross quadrotor as shown in Fig. 1.

From Fig. 1, it can be seen that the adjacent blades of the quadrotor are in opposite directions. Define the earth-frame as **E** and define the body-frame as **B**. $[\phi, \theta, \psi]^T$, $[x, y, z]^T$ and $[p, q, r]^T$ are the attitude angles associated with the earth-frame, the position in earth-frame and angular velocities related to the body-frame respectively.

For facilitating the analysis, we make the following assumption:

**Assumption 1** *Quadrotor is a rigid body, and only subjects to gravity and lift.*

The rotation matrix $C_B^E$ is used to describe the coordinate transformation and its expression is:

$$C_B^E = (\rho_{ij})_{3\times 3},$$

This work is supported in part by the National Natural Science Foundation of China under Grant 62003103, the Guangxi Natural Science Foundation under Grant 2022GXNSFBA035649, and the Interdisciplinary Scientific Research Foundation of GuangXi University under Grant 2022JCC019.

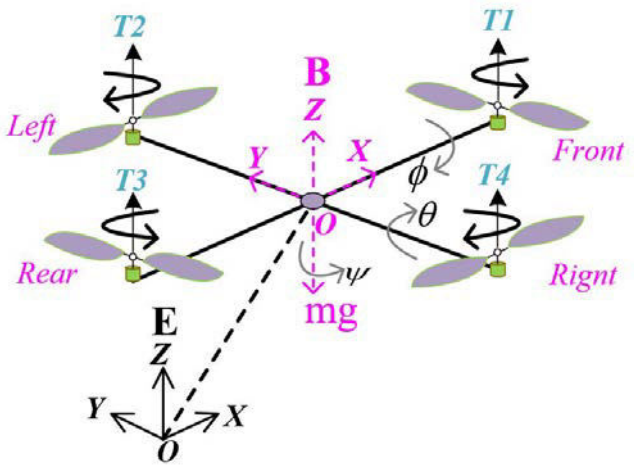


Fig. 1: Schematic diagram of the quadrotor.

where $\rho_{11} = \cos\theta\cos\phi, \rho_{12} = \sin\theta\cos\phi\sin\psi - \cos\psi\sin\phi, \rho_{13} = \sin\phi\sin\psi + \cos\phi\sin\theta\cos\psi, \rho_{21} = \cos\theta\sin\phi, \rho_{22} = \sin\theta\sin\phi\sin\psi + \cos\psi\cos\phi, \rho_{23} = \cos\phi\sin\theta\sin\psi - \cos\psi\sin\phi, \rho_{31} = -\sin\theta, \rho_{32} = \sin\psi\cos\theta, \rho_{33} = \cos\phi\cos\theta.$

### 2.2 Position model in normal equations

In the ground coordinate system, the dynamics analysis is carried out on the quadrotor. According to the second law of Newton, the quadrotor is subjected to gravity and lift, and the kinematic equation of the quadrotor can be obtained by ignoring the air resistance:

$$m\begin{bmatrix}\ddot{x}\\ \ddot{y}\\ \ddot{z}\end{bmatrix} = C_B^E\begin{bmatrix}0\\0\\T\end{bmatrix} - \begin{bmatrix}0\\0\\mg\end{bmatrix},$$

where $m$ represents the mass of the drone, $\ddot{x}$, $\ddot{y}$, $\ddot{z}$ denote the acceleration in the three-axis direction, $g$ expresses the acceleration of gravity, $T$ is the whole lifts in the body coordinate system. The lift of each rotor is calculated as follows:

$$F_i = b\Omega_i^2, i = 1, 2, 3, 4,$$

where $b$ describes the coefficient of motor, $\Omega_i$ represents the speed of the ith motor, so we get the equation of lift:

$$T = \sum_{i=1}^{4} F_i, i = 1, 2, 3, 4.$$

By sorting out the above equations, the position model of the four-rotor in geographical coordinate system can be obtained:

$$\begin{bmatrix}\ddot{x}\\ \ddot{y}\\ \ddot{z}\end{bmatrix} = \begin{bmatrix}(\sin\phi\sin\psi + \cos\phi\sin\theta\cos\psi)T/m\\ (-\cos\psi\sin\phi + \cos\phi\sin\theta\sin\psi)T/m\\ \cos\theta\cos\phi\, T/m - g\end{bmatrix}. \quad (1)$$

### 2.3 Attitude model in normal equations

According to Euler's equation, the rotational motion equation of the aircraft in the volume coordinate system is obtained:

$$M = J\cdot\mu + (\omega\times J\cdot\omega),$$

where $J$ presents the moment of inertia, $\omega$ presents the angular velocity, $\mu$ represents the angular acceleration. The angular velocity can be written as follows:

$$\omega = \begin{bmatrix}p\\q\\r\end{bmatrix}.$$

The origin of the body coordinate system coincides with the geometric center of the body, so product of inertia $J_{xy} = J_{xz} = J_{yz} = 0$, $J$ can be expressed as follow:

$$J = \begin{bmatrix}J_x & 0 & 0\\ 0 & J_y & 0\\ 0 & 0 & J_z\end{bmatrix}.$$

The total torque can be expressed as follows:

$$M = \begin{bmatrix}M_x\\M_y\\M_z\end{bmatrix} = \begin{bmatrix}l(F_1 - F_3)\\ l(F_2 - F_4)\\ a(F_1 - F_2 + F_3 - F_4)\end{bmatrix},$$

where $M_x$, $M_y$, $M_z$ are the torques on the $x$-axis, $y$-axis and $z$-axis, $a$ is a coefficient. By sorting out the above equations, the attitude model of the quadrotor as follows:

$$\begin{bmatrix}J_x\dot{p}\\ J_y\dot{q}\\ J_z\dot{r}\end{bmatrix} = \begin{bmatrix}M_x\\M_y\\M_z\end{bmatrix} + \begin{bmatrix}qr(J_y - J_z)\\ pr(J_z - J_x)\\ pq(J_x - J_y)\end{bmatrix}.$$

The relationship between the attitude angle and angular velocity of the three axes in the body coordinate system is as follows:

$$\begin{bmatrix}p\\q\\r\end{bmatrix} = \begin{bmatrix}1 & 0 & -\sin\theta\\ 0 & \cos\phi & \cos\theta\sin\phi\\ 0 & -\sin\phi & \cos\theta\cos\phi\end{bmatrix}\begin{bmatrix}\dot{\phi}\\ \dot{\theta}\\ \dot{\psi}\end{bmatrix}. \quad (2)$$

Considering the quadrotor flies at low speed and small angle, Eq (2) can be written as follows:

$$\begin{bmatrix}p\\q\\r\end{bmatrix} \approx \begin{bmatrix}\dot{\phi}\\ \dot{\theta}\\ \dot{\psi}\end{bmatrix}.$$

The attitude model is finally simplified as:

$$\begin{bmatrix}\ddot{\phi}\\ \ddot{\theta}\\ \ddot{\psi}\end{bmatrix} = \begin{bmatrix}\dot{\theta}\dot{\psi}(J_y - J_z)/J_x + U_\phi/J_x\\ \dot{\phi}\dot{\psi}(J_z - J_x)/J_y + U_\theta/J_y\\ \dot{\theta}\dot{\phi}(J_x - J_y)/J_z + U_\psi/J_z\end{bmatrix}. \quad (3)$$

### 2.4 Quadrotor 6-DOF Model

Considering the uncertainties in the system modeling, the position model (1) and the attitude model (3) can be modified as follows:

$$\begin{cases}\ddot{x} = (\sin\phi\sin\psi + \cos\phi\sin\theta\cos\psi)\cdot\frac{U_1}{m} + d_x\\ \ddot{y} = (-\cos\psi\sin\phi + \cos\phi\sin\theta\sin\psi)\cdot\frac{U_1}{m} + d_y\\ \ddot{z} = \cos\theta\cos\phi\cdot\frac{U_1}{m} - g + d_z\\ \ddot{\phi} = \dot{\theta}\dot{\psi}(J_y - J_z)/J_x + U_\phi/J_x + d_\phi\\ \ddot{\theta} = \dot{\phi}\dot{\psi}(J_z - J_x)/J_y + U_\theta/J_y + d_\theta\\ \ddot{\psi} = \dot{\theta}\dot{\phi}(J_x - J_y)/J_z + U_\psi/J_z + d_\psi\end{cases} \quad (4)$$

where $d_i (i = x, y, z, \phi, \theta, \psi)$ are unknown and bounded disturbances.

## 3 Controller design

The content of this section is to realize the target tracking of quadrotor aircraft by using sliding mode control method. The designed block diagram of control system is shown in Fig. 2. The position control loop and attitude control loop are designed to force the actual position $[x, y, z]$ and attitude $[\phi, \theta, \psi]$ to reach the desired position $[x_d, y_d, z_d]$ and attitude $[\phi_d, \theta_d, \psi_d]$. The double closed-loop is closely connected with the attitude solution module to complete the control of the controlled object.

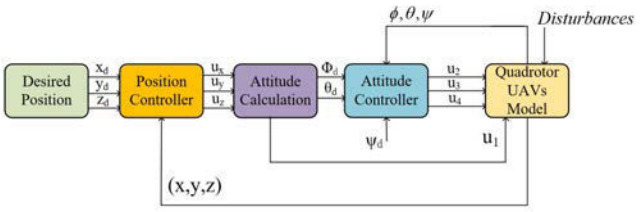


Fig. 2: Control block diagram of the quadrotor.

### 3.1 Position controller design

Noting that $U_1$ directly determines the height of the quadrotor in the position control process, the horizontal displacement control quantities in directions $x$, $y$ and height control quantity are derived as follows:

$$\begin{cases} U_x = (\sin\phi\sin\psi + \cos\phi\sin\theta\cos\psi)\cdot U_1/m \\ U_y = (-\cos\psi\sin\phi + \cos\phi\sin\theta\sin\psi)\cdot U_1/m \\ U_z = U_1\cdot\cos\phi\cos\theta/m - g \end{cases} \quad (5)$$

Since the control inputs $U_i$, $i = x, y, z, \phi, \theta, \psi$ are constrained in the reality, the saturated input is considered as

$$U_i = sats(U_i^{'}),\ i = x,\ y,\ z,\ \phi,\ \theta,\ \psi, \quad (6)$$

where the $sats(U_i^{'})$ is defined as:

$$sats(U_i^{'}) = \begin{cases} U_{max}, U_i^{'} > U_{max} \\ U_i^{'}, \mid U_i^{'} \mid \leq U_{max} \\ -U_{max}, U_i^{'} < -U_{max} \end{cases},$$

where $U_{max}$ is a positive constant and $U_i^{'}$ is unlimited control input. Noting that $U_i^{'}$ is bounded in practical systems. Then there is an unknown function $\delta_i$ such that:

$$U_i = U_i^{'} + \delta_i, \quad (7)$$

Herein, we design an adaptive law to estimate $\delta_i$ which has the following form:

$$\dot{\hat{\delta}}_i = \rho_i S_i,\ i = x,\ y,\ z,\ \phi,\ \theta,\ \psi. \quad (8)$$

On the other hand, we adopt sliding mode control strategies to achieve a desired tracking performance. In the present paper, the sliding surface $S_1$ is selected as:

$$S_1 = \begin{bmatrix} S_x \\ S_y \\ S_z \end{bmatrix} = \begin{bmatrix} \dot{e}_x + c_1 e_x \\ \dot{e}_y + c_2 e_y \\ \dot{e}_z + c_3 e_z \end{bmatrix}, \quad (9)$$

where $c_1 > 0, c_2 > 0, c_3 > 0$ are control parameters to be specified, and the tracking error $e_1$ is:

$$e_1 = \begin{bmatrix} e_x \\ e_y \\ e_z \end{bmatrix} = \begin{bmatrix} x - x_d \\ y - y_d \\ z - z_d \end{bmatrix}.$$

Based on Eq (9), taking the first-order derivative of the sliding surface $S_1$ yields:

$$\dot{S}_1 = \begin{bmatrix} \dot{S}_x \\ \dot{S}_y \\ \dot{S}_z \end{bmatrix} = \begin{bmatrix} \ddot{e}_x + c_1\dot{e}_x \\ \ddot{e}_y + c_2\dot{e}_y \\ \ddot{e}_z + c_3\dot{e}_z \end{bmatrix} = \begin{bmatrix} (U_x + d_x) - \ddot{x}_d + c_1\dot{e}_x \\ (U_y + d_y) - \ddot{y}_d + c_2\dot{e}_y \\ (U_z + d_z) - \ddot{z}_d + c_3\dot{e}_z \end{bmatrix}. \quad (10)$$

In order to ensure that the sliding mode surface can be reached from any states in finite time, we adopt the method of exponential reaching law:

$$U_{sw} = -k_i \mathrm{sgn}(S_i) - h_i S_i,$$

where $h_i > 0, k_i > \mid d_i \mid (i = x, y, z)$, so as to overcome the disturbance. Thus, the position control law is obtained as:

$$\begin{cases} U_x^{'} = \ddot{x}_d - c_1\dot{e}_x - k_x\mathrm{sgn}(S_x) - h_x S_x - \hat{\delta}_x \\ U_y^{'} = \ddot{y}_d - c_2\dot{e}_y - k_y\mathrm{sgn}(S_y) - h_y S_y - \hat{\delta}_y \\ U_z^{'} = \ddot{z}_d - c_3\dot{e}_z - k_z\mathrm{sgn}(S_z) - h_z S_z - \hat{\delta}_z \end{cases}. \quad (11)$$

### 3.2 Attitude controller design

We calculate the expected angle input of attitude loop according to position loop. From Eq (5), ones obtain:

$$\begin{bmatrix} U_x \\ U_y \end{bmatrix} = \begin{bmatrix} \cos\psi & \sin\psi \\ \sin\psi & -\cos\psi \end{bmatrix} \begin{bmatrix} \sin\theta\cos\phi \\ \sin\phi \end{bmatrix} U_1/m,$$

where $U_1 = m\sqrt{(U_z + g)^2 + U_x^2 + U_y^2}$, The above equality yields that:

$$\begin{cases} \theta_d = \arctan\left(\frac{\cos\psi_d U_x + \sin\psi_d U_y}{U_z + g}\right) \\ \phi_d = \arctan\left(-\frac{\cos\psi_d U_y - \sin\psi_d U_x}{U_z + g}\cos(\theta_d)\right) \end{cases}.$$

Then we define the sliding mode surface $S_2$ as:

$$S_2 = \begin{bmatrix} S_\phi \\ S_\theta \\ S_\psi \end{bmatrix} = \begin{bmatrix} \dot{e}_\phi + c_4 e_\phi \\ \dot{e}_\theta + c_5 e_\theta \\ \dot{e}_\psi + c_6 e_\psi \end{bmatrix}, \quad (12)$$

where $c_4 > 0, c_5 > 0, c_6 > 0$ are control parameters, and the path error $e_2$ is:

$$e_2 = \begin{bmatrix} e_\phi \\ e_\theta \\ e_\psi \end{bmatrix} = \begin{bmatrix} \phi - \phi_d \\ \theta - \theta_d \\ \psi - \psi_d \end{bmatrix}.$$

Based on Eq (12), taking the first-order derivative of the sliding mode surface $S_2$ yields:

$$\dot{S}_2 = \begin{bmatrix} \dot{S}_\phi \\ \dot{S}_\theta \\ \dot{S}_\psi \end{bmatrix} = \begin{bmatrix} \ddot{e}_\phi + c_4\dot{e}_\phi \\ \ddot{e}_\theta + c_5\dot{e}_\theta \\ \ddot{e}_\psi + c_6\dot{e}_\psi \end{bmatrix}. \quad (13)$$

Substituting Eq (3) into Eq (13) to get the following equations, taking the first-order derivative of the sliding surface

$S_2$ yields:

$$\begin{cases} \dot{S}_\phi = \frac{\dot{\theta}\dot{\psi}(J_y - J_z)}{J_x} + \frac{U_\phi^{'} + \delta_\phi}{J_x} + d_\phi - \ddot{\phi}_d + c_4\dot{e}_\phi \\ \dot{S}_\theta = \frac{\dot{\phi}\dot{\psi}(J_z - J_x)}{J_y} + \frac{U_\theta^{'} + \delta_\theta}{J_y} + d_\theta - \ddot{\theta}_d + c_5\dot{e}_\theta \\ \dot{S}_\psi = \frac{\dot{\phi}\dot{\psi}(J_x - J_y)}{J_z} + \frac{U_\psi^{'} + \delta_\psi}{J_z} + d_\psi - \ddot{\psi}_d + c_6\dot{e}_\psi \end{cases}.$$

By using the method of exponential reaching law, the controllers for the attitude loop can be acquired as follows:

$$\begin{cases} U_\phi^{'} = J_x\big(\ddot{\phi}_d - c_4\dot{e}_\phi - k_4\mathrm{sgn}(S_\phi) - h_\phi S_\phi \\ \qquad - \frac{\dot{\theta}\dot{\psi}(J_y - J_z)}{J_x}\big) - \hat{\delta}_\phi \\ U_\theta^{'} = J_y\big(\ddot{\theta}_d - c_5\dot{e}_\theta - k_\theta\mathrm{sgn}(S_\theta) - h_\theta S_\theta \\ \qquad - \frac{\dot{\phi}\dot{\psi}(J_z - J_x)}{J_y}\big) - \hat{\delta}_\theta \\ U_\psi^{'} = J_z\big(\ddot{\psi}_d - c_6\dot{e}_\psi - k_\psi\mathrm{sgn}(S_\psi) - h_\psi S_\psi \\ \qquad - \frac{\dot{\phi}\dot{\psi}(J_x - J_y)}{J_z}\big) - \hat{\delta}_\psi \end{cases} \tag{14}$$

### 3.3 Stability analysis

Based on the above analysis, the main result is summarized as follows.

**Theorem 1** Consider the dynamical model of quadrotors (4) with saturated input (6). If the controllers and the adaptive laws are designed as (11), (14) and (8), then the following statements hold:

i) All signals of the position-loop system are bounded;
ii) The tracking errors converge to zeros asymptotically.

**Proof.** Noting that the position model and the attitude model in the closed-loop systems are decoupled. We first analyze the stability of position model. Choosing the Lyapunov function $V_p$ for the position model, which is defined as:

$$V_p = \frac{1}{2}S_x^2 + \frac{1}{2}S_y^2 + \frac{1}{2}S_z^2 + \frac{1}{2\rho_x}\tilde{\delta}_x^2 + \frac{1}{2\rho_y}\tilde{\delta}_y^2 + \frac{1}{2\rho_z}\tilde{\delta}_z^2.$$

where $\tilde{\delta}_i = \hat{\delta}_i - \delta_i, \dot{\delta}_i = 0, \rho_i > 0, i \in \{x, y, z\}$.

Taking the derivative of $V_p$ along with the position subsystem:

$$\begin{aligned} \dot{V}_p =& S_x\dot{S}_x + S_y\dot{S}_y + S_z\dot{S}_z + \frac{1}{\rho_x}\tilde{\delta}_x\dot{\tilde{\delta}}_x + \frac{1}{\rho_y}\tilde{\delta}_y\dot{\tilde{\delta}}_y + \frac{1}{\rho_z}\tilde{\delta}_z\dot{\tilde{\delta}}_z \\ =& S_x(-k_x\mathrm{sgn}(S_x) - h_xS_x - \tilde{\delta}_x + d_x) + S_y(-k_y\mathrm{sgn}(S_y) \\ & -h_yS_y - \tilde{\delta}_y + d_y) + S_z(-k_z\mathrm{sgn}(S_z) - h_zS_z - \tilde{\delta}_z + d_z) \\ & + \frac{1}{\rho_x}\tilde{\delta}_x\dot{\tilde{\delta}}_x + \frac{1}{\rho_y}\tilde{\delta}_y\dot{\tilde{\delta}}_y + \frac{1}{\rho_z}\tilde{\delta}_z\dot{\tilde{\delta}}_z \\ =& S_xd_x - k_x \mid S_x \mid - h_xS_x^2 + S_yd_y - k_y \mid S_y \mid - h_yS_y^2 \\ & + S_zd_z - k_z \mid S_z \mid - h_zS_z^2 + \tilde{\delta}_x(\frac{\dot{\tilde{\delta}}_x}{\rho_x} - S_x) \\ & + \tilde{\delta}_y(\frac{\dot{\tilde{\delta}}_y}{\rho_y} - S_y) + \tilde{\delta}_z(\frac{\dot{\tilde{\delta}}_z}{\rho_z} - S_z) \end{aligned} \tag{15}$$

Substituting Eq (8) into Eq (15), we get:

$$\begin{aligned} \dot{V}_p \leq & \mid S_x \mid (\mid d_x \mid - k_x) + \mid S_y \mid (\mid d_y \mid - k_y) \\ & + \mid S_z \mid (\mid d_z \mid - k_z) < 0, \end{aligned}$$

which means that the signals $S_i$, $\tilde{\delta}_i$, $i \in \{x, y, z\}$ of the position subsystem are bounded, and the tracking error $e_1$ converges to zero asymptotically. Moreover, since $|\hat{\delta}_i| = |\hat{\delta}_i - \delta_i + \delta_i| \leq |\tilde{\delta}_i| + |\delta_i| < +\infty, i \in \{x, y, z\}$. It concludes that all signals of the closed-loop systems are bounded.

For the attitude subsystem, it can be proved in the similar way. The detailed proof is omitted here. ■

**Remark1:** Considering that chatttering will occur in C-SMC due to time delay and space lag, etc. We replace the symbol function $sign(s)$ with the saturation function $\chi(s)$, so that the state points can be limited near the sliding mode surface, which can weaken chattering. The saturation function is chosen as:

$$\chi(s) = \begin{cases} 1, s > \zeta \\ \frac{1}{\zeta} \cdot s, |s| \leq \zeta \\ -1, s < -\zeta \end{cases},$$

where $\zeta$ is the limiting layer, and inside limiting layer is the continuous control.

## 4 Simulation Results

We will verify the effectiveness of the control laws in this section. By building a simulation environment, we will track the path of the quadrotor and analyze the results. The parameters of the selected quadrotor are shown in Table 1.

Table 1: Parameters values of the quadrotor

| symbol | value | physical meaning |
|---|---|---|
| m | 1.5 | Mass of the quadrotor(Kg) |
| l | 0.225 | Arm length(m) |
| g | 9.8 | Gravitational acceleration($\mathrm{m/s^2}$) |
| $\mathrm{J}_{xx}$ | 0.0211 | Moment of inertia on $x$-axis($\mathrm{Kg.m^2}$) |
| $\mathrm{J}_{yy}$ | 0.0212 | Moment of inertia on $y$-axis($\mathrm{Kg.m^2}$) |
| $\mathrm{J}_{zz}$ | 0.0366 | Moment of inertia on $z$-axis($\mathrm{Kg.m^2}$) |

We set the initial attitude angle $[\phi, \theta, \psi]$ and position $[x, y, z]$ of the quadrotor as zero. Firstly, we set the expected yaw angle $\psi = \frac{\pi}{6}$ and the expected position as fixed point [3,3,3]. In order to better verify that the system is invariant to external disturbances under SMC, we choose the common sine function to represent disturbances as follows:

$$d_i = m_i \cdot \sin(t), (i = x, y, z, \phi, \theta, \psi),$$

perturbed the two subsystems with different interfernce, where $m_x = m_y = m_z = 0.1, m_\phi = m_\theta = m_\psi = 0.3$.

After repeated debugging, the parameters of the controller are: $c_1 = c_2 = c_3 = 3, k_x = k_y = k_z = 1.7, h_x = h_y = h_z = 1, c_4 = c_5 = c_6 = 3.5, k_\theta = k_\theta = k_\psi = 2.5, h_\theta = h_\theta = h_\psi = 2.5, \zeta = 0.4, \rho_i = 0.05$.

We give a restricted range of four control inputs as follow:

$$|U_1| \leq 22, |U_i| \leq 1 (i = 2, 3, 4).$$

It can be seen from Fig. 3 that the AQSMC has better control accuracy and speed. Although the response speed of the PID control is very fast, AQSMC will reach the desired signal stably within finite time. Similarly, in Fig. 4, in the process of dynamic change of roll angle and pitch angle, AQSMC changes very little at the beginning, which can

satisfy the hypothesis of small angle change. With the pitch angle given externally, the PID effect is still not ideal. From the figures, AQSMC can achieve better quadrotor fixed-point hover effect.

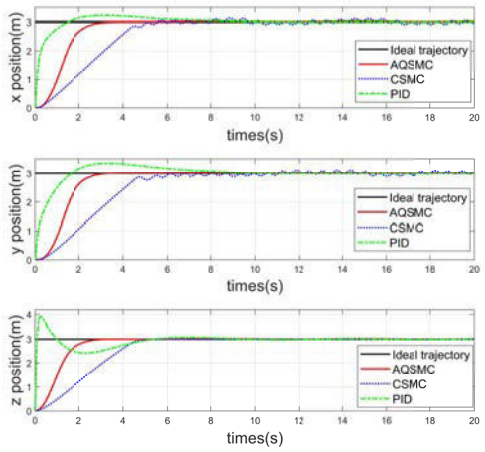


Fig. 3: Position trajectory tracking.

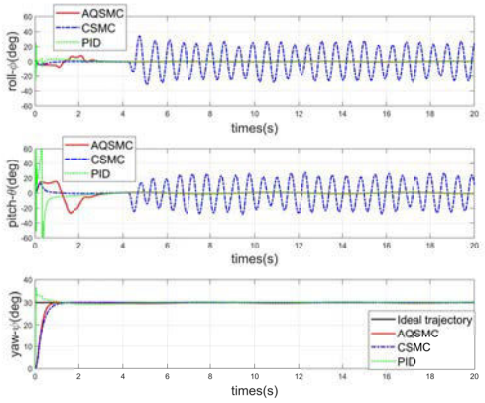


Fig. 4: Attitude trajectory tracking.

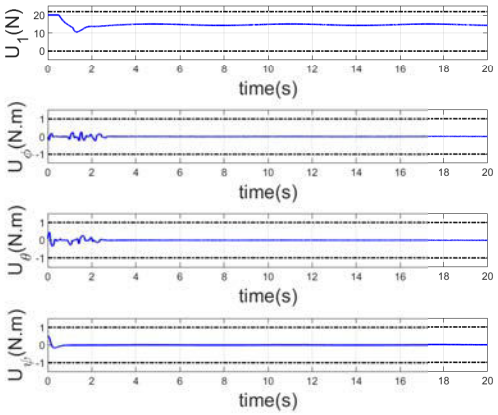


Fig. 5: Control inputs with AQSMC.

Fig. 5 and 10 show that the limited actual control inputs, they do not have excessive gain. Fig. 6 and 11 show that the

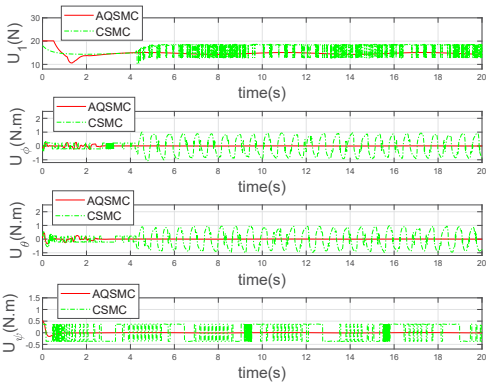


Fig. 6: Control inputs comparison.

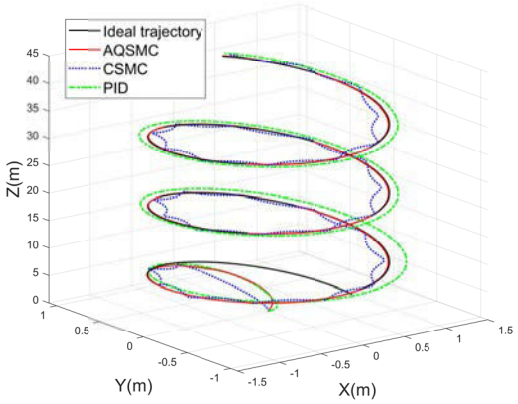


Fig. 7: Flight around in circle.

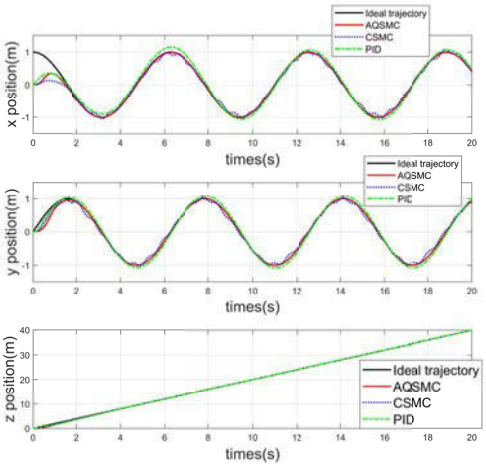


Fig. 8: Position trajectory tracking of flight around in circle.

AQSMC inhibited chattering better than CSMC. CSMC produces excessive gain, which can damage hardware in reality. Furthermore, time-dependent circular trajectory is used to track the trajectory again, another expected trajectory is implemented:

$$\xi_d(t) = [\cos t, \sin t, 2t].$$

Similarly, control parameters and external disturbances remain unchanged. Fig. 7-9 are the result of dynamic trajectory tracking, it can be seen from the results that QSMC still has a good effect.

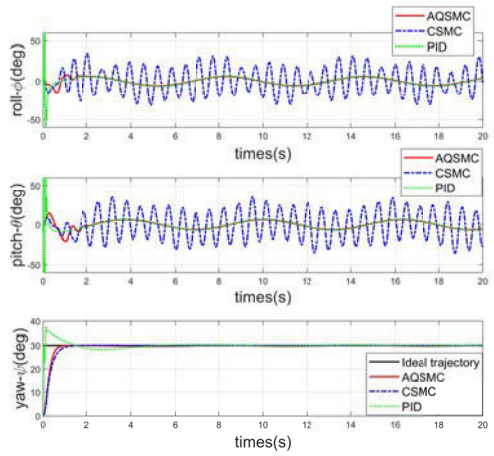


Fig. 9: Attitude trajectory tracking of flight around in circle.

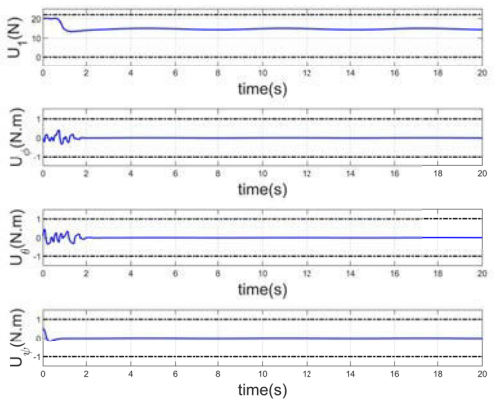


Fig. 10: Control inputs with AQSMC.

## 5 Conclusion

An adaptive quasi-sliding mode control algorithm has been proposed to achieve the position and attitude tracking control of quadrotors with input saturation and unknown bounded uncertainties. The stability of the closed-loop system was proved by the Lyapunov direct method. The merit of the proposed control approach is improved tracking speed and accuracy, and ensures robustness and low-gain inputs compared with traditional methods, such as conventional SMC and PID. Simulation has confirmed the effectiveness of the proposed results.

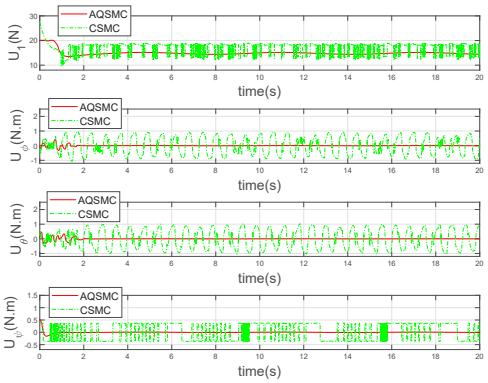


Fig. 11: Control inputs comparison.

## References


[1] H. Eisenbeiss, A mini unmanned aerial vehicle system overview and image acqusition. In *Proc. International Workshop On Processing And Visualization Using High Resolution Imagery*, 2009.

[2] J. J. Xiong, E. H. Zheng, Position and attitude tracking control for a quadrotor UAV. *ISA Trans*, 53(3): 725–731, 2014.

[3] L. Guettal, H. E. Glida, and A. Chelihi, Adaptive fuzzy-neural network based decentralized backstepping controller for attitude control of quadrotor helicopter. In *2020 1st International Conference on Communications, Control Systems and Signal Processing (CCSSP)*, 394–399, 2020.

[4] W. Lei, C. Li, and Z. Q. M. Chen, Robust adaptive tracking control for quadrotors by combining PI and self-tuning regulator. *IEEE Trans. Control Syst. Technol*, 27(6): 2663–2671, 2019.

[5] K. Nonami, K. Den, Sliding mode control. Tokyo:Corona Publishing. 1994.

[6] W. Shang, G. Jing, D. Zhang, T. Chen, and Q. Liang, Adaptive fixed time nonsingular terminal sliding-mode control for quadrotor formation with obstacle and inter-quadrotor avoidance. *IEEE Access*, 60640–60657, 2021.

[7] Z. Li, G. Yu, Q. Zhang, S. Song, and H. Cui, Adaptive sliding mode control for spacecraft rendezvous with unknown system parameters and input saturation. *IEEE Access*, 9: 67724–67733, 2021.

[8] V. Nekoukar, N. M. Dehkordi, Robust path tracking of a quadrotor using adaptive fuzzy terminal sliding mode control. *Control Eng. Practice*, 110: 104763, 2021.

[9] R. J. Wai, K. H. Su, Adaptive fuzzy sliding-mode control for electrical servo drive. *IEEE Trans. Ind. Electron*, 53(2), 569–580, 2006.

[10] Y. Li, D. Wang, Servo motor sliding mode control based on fuzzy power index method. *Comput. Electr. Eng*, 94: 107351, 2021.

[11] S. C. Yogi, V. K. Tripathi, and L. Behera, Adaptive integral sliding mode control using fully connected recurrent neural network for position and attitude control of quadrotor. *IEEE Trans. Neural Netw. Learn. Syst*, 32(12): 5595–5609, 2021.

[12] V. Utkin, H. Lee, Chattering Problem in Sliding Mode Control Systems. in *Proc.2006 Int. Workshop Variable Structure Syst.*, Alghero, Italy, Jun. 5-7, 346–350, 2006.